MNRAS **000**, 1–15 (2020) Preprint 15 September 2020 Compiled using MNRAS LATEX style file v3.0

Asteroseismology of *SZ Lyn* using Multi-Band High Time Resolution Photometry from Ground and Space

J. Adassuriya[1⋆], S. Ganesh[2], J. L. Gutiérrez[3], G. Handler[4], Santosh Joshi[5]
K. P. S. C. Jayaratne[6], K. S. Baliyan[2]
[1]*Astronomy Division, Arthur C Clarke Institute, Colombo, Sri Lanka*
[2]*Astronomy and Astrophysics Division, Physical Research Laboratory, Ahmedabad, India*
[3] *Department of Physics, Universitat Politecnica de Catalunya, Castelldefels, Spain*
[4]*Nicolaus Copernicus Astronomical Center, Bartycka 18, 00-716 Warsaw, Poland*
[5]*Aryabhatta Research Institute of Observational Sciences (ARIES), Manora Peak-Nainital, India*
[6]*Department of Physics, University of Colombo, Colombo, Sri Lanka*

Accepted XXX. Received YYY; in original form ZZZ

ABSTRACT

We report the analysis of high temporal resolution ground and space based photometric observations of SZ Lyncis, a large amplitude δ Scuti type binary. UBVR photometry were obtained from Mt. Abu Infrared Observatory, Fairborn Observatory and the Wide Angle Search for Planets program as well as continuous light curve from the Transiting Exoplanet Survey Satellite project. The well resolved light curves reveal the possible presence of 23 frequencies with four independent modes, 13 harmonics of the main pulsation frequency of 8.296943 ± 0.000002 cycles/day (c/d) and their combinations. The frequency 8.296 c/d is identified as the fundamental radial mode by amplitude ratio method and using the estimated pulsation constant. The frequencies 14.535, 32.620 and 4.584 c/d are newly discovered for SZ Lyn. Out of these three, 14.535 and 32.620 c/d are identified as non-radial lower order p-modes and 4.584 c/d is identified as a g-mode which confirmed the presence of scarce pulsation spectrum in δ Scuti stars. As a result of frequency determination and mode identification, the physical parameters of SZ Lyn were revised by optimizations of stellar pulsation models with the observed frequencies. The best theoretical model correspond to $T_{\rm eff}$=7557 K, $\log(g)$ = 3.86, and R=2.86 $R_\odot$. The mass of SZ Lyn was estimated to be close to 1.9±0.1 $M_\odot$ using evolutionary models. The period-density relation estimates a mean density ρ of 0.1054±0.0016 g cm^{-3}.

Key words: asteroseismology, techniques: photometry, stars: variables: δ Scuti, stars: individual: SZ Lyn, stars: fundamental parameters

1 INTRODUCTION

The study of multi-periodic stellar pulsations represents a unique methodology for studying the interior of a star (Bowman et al. 2018). The pulsation in stars could be either radial and/or non-radial in nature and is driven through either pressure waves (p-mode) or gravity waves (g-mode). In p-modes, pressure is the primary restoring force for a star perturbed from equilibrium, while in g-mode, buoyancy is the restoring force (Aerts et al. 2010). Diverse pulsation group includes Beta Cephei (β Cep), slowly pulsating B (SPB) stars, gamma Doradus (γ Dor), δ Scuti etc. Garrido et al. (1990), Breger (2000b), Handler et al. (2006), Handler (2008) provide detailed discussion on the ground based observations of these stars. The group of δ Scuti is located in the region where the classical instability strip intersects to the main sequence in the Hertzsprung-Russell (HR) diagram. Their spectral range is from A2 to F0 corresponding to temperatures of 7000 K < T_{eff} < 9300 K (Uytterhoeven et al. 2011). Typical periods for p-mode pulsations in δ Scuti stars range from 15 min to 5 h (Uytterhoeven et al. 2011). These stars are of intermediate mass ranging between 1.5 to 2.5 $M_\odot$ (Aerts et al. 2010), hence most of them are in the core hydrogen burning or shell hydrogen burning phase and possess convective cores. See Breger (2000b) for a detailed discussion on these stars. Furthermore, the δ Scuti type pulsations have been detected in many pre- and post-main sequence (Antoci et al. 2019) stars while low amplitude δ Scuti type pulsations have been detected in many metallic A-type (Am) stars (Joshi et al. 2012, 2016, 2017). The com-

⋆ E-mail:adassuriya@gmail.com

Table 1. Physical parameters of SZ Lyn derived in literature. The parameters were used to generate pulsation and evolutionary models of SZ Lyn.

Parameter	Value	Reference
T_{eff} (K)	7540	Langford (1976)
	7235	LAMOST
	7799	Gaia
log(g)	3.88	Langford (1976)
	3.94	LAMOST
Mass ($M_\odot$)	1.57(+0.17)	Fernley et al. (1984)
Radius ($R_\odot$)	2.76	Fernley et al. (1984)
	2.80	Bardin & Imbert (1981)
Parallax (mas)	2.49±0.07	Gaia

plex interior structures of these stars can only be examined by a study of the multi-periodic radial and non-radial pulsation modes, a technique known as asteroseismology (Aerts et al. 2010; Joshi & Joshi 2015).

In this paper, we present a detailed analysis of SZ Lyncis, HD 67390 (RA=08h 09m 35.8s, DEC=+44° 28′ 17.6″) a High Amplitude δ Scuti (HADS) type binary star, m_v= 9.1, with reported pulsation and orbital period 0.12053793 days and 1173.5 days, respectively (Soliman et al. 1986). SZ Lyn is a brighter component of the binary system where the fainter component is not observed with spectroscopic technique; hence characterized as a single line spectroscopic binary (Gazeas et al. 2004). The fundamental pulsation period of this star was first determined by Binnendijk (1968) and later refined by Gazeas et al. (2004).

SZ Lyn has been studied on a number of occasions for the orbital and pulsation parameters. Van Genderen (1967) reported that the linear ephemeris for the time of pulsation maximum has not been accurately estimated. Barnes III & Moffett (1975) suggested that the very long period orbital motion of SZ Lyn affected the linear ephemeris due to the light-travel time across the orbit. Using photometric and spectroscopic data, Moffett et al. (1988) introduced a non-linear ephemeris for the times of light maxima and determined improved values for the pulsation and orbital parameters. A similar analysis was made by Paparó et al. (1988) and Li & Qian (2013). The observed minus calculated (O-C) diagrams show periodic as well as secular variations, and (Paparó et al. 1988) concluded that the main pulsation period changes by $(2.25 \pm 0.42) \times 10^{-12}$ day per cycle. This value was later refined as $(2.90 \pm 0.22) \times 10^{-12}$ day per cycle by Gazeas et al. (2004).

The physical parameters (see Table 1) of SZ Lyn have been determined by several authors. This star has nearly solar abundance (Alania 1972; Langford 1976) with mean temperature of 7540 K and log(g) of 3.88 (Langford 1976). The multi-band light curves inferred radius of 2.76 $R_\odot$ and mass 1.57 $M_\odot$ (Fernley et al. 1984). Using high time resolution radial velocity curves, Bardin & Imbert (1981) determined the stellar atmospheric displacement as 0.115 $R_\odot$ assuming the radius to be 2.8 $R_\odot$. Further studies reported by Bardin & Imbert (1981) determined the radial velocity of SZ Lyn as 30 km/s. The Large Sky Area Multi-Object Fiber Spectroscopic Telescope (LAMOST) has observed SZ Lyn in low resolution spectroscopic mode and determined T_{eff}=7235 K, and log(g)=3.94. *Gaia* (Gaia Collaboration et al. 2016, 2018; Luri et al. 2018) determined a parallax of 2.49 ± 0.07 milliarcseconds, placing at a distance of $401.6^{+11.6}_{-11.0}$ pc. Most of the previous works reported the main pulsation period and few a attempts have also been made to search for additional harmonics and secondary pulsation periods. Apart from the main pulsation period, two harmonics of the fundamental period were reported by Gazeas et al. (2004).

Here, we have subjected SZ Lyn for the asteroseismic analysis. Using the higher temporal multi-band light curves from ground and highly-precise photometric data from space mission, we attempted to find more frequencies in SZ Lyn and identify the pulsation modes, l. The manuscript is organised as follows: The observational data and reduction procedures are given in Sec. 2. The frequency analysis is performed in Sec. 3. In Sec. 4, the mode identification procedures are discussed in detail paying special attention to the theoretical model analysis. The refinement of stellar parameters of SZ Lyn is presented in Sec. 5 followed by the evolutionary and pulsation models. Finally, we have discussed the results with a detailed consideration of the limitations of our analysis in Sec. 6 and summarized the results under Sec 7.

2 PHOTOMETRIC OBSERVATIONS

Imaging data from various sources (Mount Abu, APT, WASP and TESS) are included in the current study. The Table 2 compiles the observing log along with details of the filter used, the cadence, number of nights, and the total number of data points. In the following subsections, the data are further described.

2.1 Mount Abu

A series of observations were carried out from Mt. Abu InfraRed Observatory (MIRO). The observatory is located at the highest peak, Gurushikhar, of Aravali range near Mount Abu in the western state of Rajasthan, India. The observatory is located at 24.65° N, 72.78° E, at an altitude of 1680 meters where one can obtain typical seeing ∼1.2 arc seconds.

Observations were made with the Corrected Dall-Kirkham (CDK) 50 cm, f/6.8 equatorial mount telescope equipped with an Andor 1024×1024 EMCCD, thermo-electrically cooled to −80°C. Details about the setup are provided by Ganesh et al. (2013). The higher frame rates and negligible read out noise (<1 electron with EM gain), characteristic of EMCCD, are ideal for the observation of short period variable stars with high cadence. The large EMCCD array provides a field of view of 13×13 arc minutes. The system was fully automated and the exposures were scripted using RTS2[1] which allowed to obtain repeated sequences of B, V and R single frames with different exposure times for each filter. The filter movement being automated, very little time is lost in this process. After removing faulty frames, we have acquired a total of 4328 frames in B, 4569 in V and 6836 in R during the seven nights of observation between December 2013 and

[1] RTS2 : Remote Telescope System v2 is available at http://rts2.org/

November 2016(see Table 2). At least one pulsation cycle of SZ Lyn was covered in B, V and R on each night.

The basic reduction procedures of the Mount Abu data were performed using the IRAF[2] software. All the frames were brought to a common centre before extraction of instrumental magnitudes. The alignment was done using *imcentroid* and *imshift* tasks in IRAF. The average deviation of the frames after the centering is 0.52 pixels in x direction and 0.17 pixels in y direction which is equivalent to 0.50 arc seconds and 0.13 arc seconds, respectively. This accurate alignment of all the images improves the signal to noise ratio as well as eliminates any magnitude variations due to imperfect aperture centering. The photometry was performed by running the *phot* package in IRAF. The instrumental magnitudes were extracted for the BVR bands using an aperture of size 3 to 4 times the FWHM of program star for different filters. An annulus of 5 pixels width was used for all the bands to determine the background. Two stars of magnitudes m_V= 10.5 (TYC 2979-1329) and m_V= 10.8 (TYC 2979-1343), in the same field of view were used as comparison stars for differential photometry in each band.

The colour variations (B-V) and (V-R) were determined for the Mount Abu data. Since the time series observations were taken in consecutive B, V and R bands, spline interpolation was performed on the light curves to obtain simultaneous values in all filter bands. The B and R band data were fitted by means of a cubic spline interpolation and the coefficients of the spline were calculated. Then B and R magnitudes were determined for the time stamps of V band to get the magnitudes of B and R at the same time as V. The amplitude of the variations of SZ Lyn in the BVR bands were $\Delta B \sim 0.7$, $\Delta V \sim 0.5$ and $\Delta R \sim 0.4$ magnitudes. Both colour and magnitude variations reveal that magnitude change in B is the highest, as expected for a δ Scuti star. Therefore, B band was used as the reference filter in the UBVR system for the calculation of observed and theoretical amplitude ratios presented in Sec. 4.

2.2 APT

Differential time-series photoelectric data were collected through the Johnson UBV filters with the 0.75 m Automatic Photoelectric Telescope (APT) T6 at Fairborn Observatory in Arizona (Strassmeier et al. 1997). Two comparison stars, HD 67808 and HD 66113, were used. Integration times were 2 × 20 s in each filter, with the exception of the U filter for SZ Lyn in which an integration time of 2 × 30 s was used to collect enough photons.

The data were reduced following standard photoelectric photometry schemes. First, the measurements were corrected for coincidence losses. Then, sky background was subtracted within each target/local comparison star group. Standard extinction coefficients were employed; small errors in their assumption would be compensated when computing differential magnitudes. Obviously, the same extinction correction was applied to each star. Some bad measurements due to partly poor telescope tracking had to be eliminated. Finally, differential magnitudes were computed by interpolation, and the timings were converted to Heliocentric Julian Date. During the reductions it turned out that HD 66113 could be a low-amplitude δ Scuti star (f = 12.573 d^{-1}, A_V = 2.1 mmag), hence it was rejected from the computation of the differential light curves of SZ Lyn. We obtained a total of 701/688/672 good measurements for the U, B, and V filters, respectively, with an estimated accuracy of 4.5/3.5/3.5 mmag per point. The time span of the combined data set is 35.05 d, with data collected on 24 nights.

2.3 WASP

The Wide Angle Search for Planets (WASP) observatories consist of two identical robotic telescopes, one located at La Palma and other at South African Astronomical Observatory (Pollacco et al. 2006). The WASP program also observed SZ Lyn during the period March 2007 to April 2008 in its own wide pass-band (Table 2). Two exposures of each field with 30 seconds were obtained, and each field was sampled every 9–12 minutes, totalling 2894 data points with 216 effective hours of observation. The flux were converted to magnitudes by the WASP (Butters et al. 2010) so that the light curve in Fig. 1 is in magnitude scale. The WASP data are neither equally distributed nor differential, and the differential magnitudes from the APT data were computed with respect to a much brighter and bluer star than Mount Abu data. Furthermore, the filter bandpasses of the three ground based data sources are different. Due to these inconsistencies between the ground data, we refrained from combining all three data sources into a single light curve and hence the analyses were performed separately.

2.4 TESS

SZ Lyn was observed by TESS (Ricker et al. 2015) in sector 20, ID number TIC 192939152, from 24$^{\rm th}$ December 2019 to 19$^{\rm th}$ January 2020 in 120 seconds of cadence. The light curves were generated using simple aperture photometry and corrected by pre-search data conditioning (PDC). The PDC pipeline module uses singular value decomposition to identify and correct for time-correlated instrumental signatures such as, spacecraft pointing jitter, long-term pointing drifts due to differential velocity aberration, and other stochastic errors (Jenkins et al. 2016; Balona et al. 2019). The corrected flux from TESS Asteroseismic Science Operation Center (TASOC) were converted to magnitudes. A part of light curve of each data source for the duration of 0.25 days is shown in Fig. 1. The power spectra on the right side in the same figure are a good comparison of resolving power of frequencies of the ground and space based data.

3 FREQUENCY ANALYSIS

For seismic analysis, the light curves observed from Mount Abu, APT WASP and TESS data were searched for frequencies independently. We used the generalized Lomb-Scargle (LS) (Zechmeister & Kürster 2009) algorithm since ground

[2] IRAF is distributed by the National Optical Astronomy Observatory, which is operated by the Association of Universities for Research in Astronomy (AURA) under a cooperative agreement with the National Science Foundation.

Table 2. Photometric observation of SZ Lyn. The JD column shows exact date of observation at Mount Abu and the observation periods of the other three data sources.

Observation	JD (2450000)	Effective nights	Band	Coverage (h)	Cadence (s)	Data points
Mount Abu (India)	6639.104 6640.153 6664.134 6684.118 6686.174 6693.097 7705.135	7	B V R	29.2 28.9 55.3	5 2 2	4328 4569 6836
APT (USA)	7480.634-7515.688	24	U B V	50.1 51.4 52.5	60 40 40	701 688 672
WASP	4190.366-4575.408	39	(400-750) nm	216.0	60	2894
TESS	8842.503-8868.827	25 (days)	(600-1000) nm	631.8	120	16550

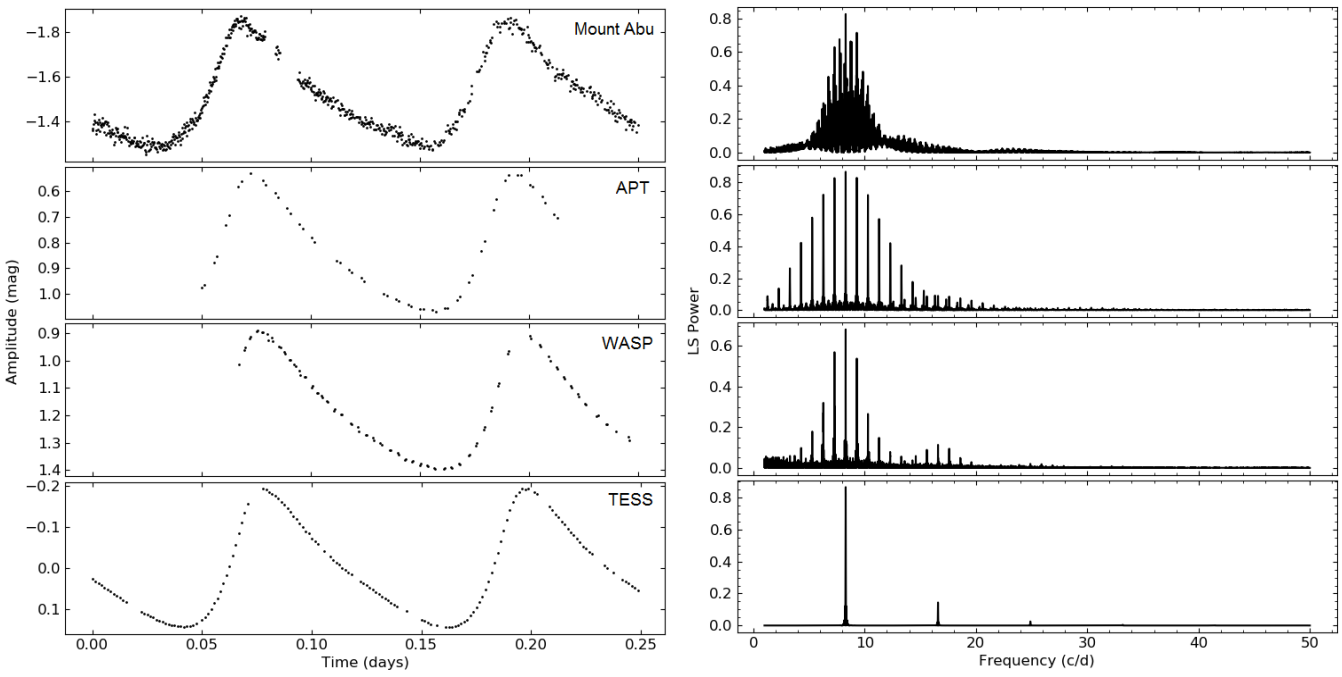

Figure 1. The high cadence light curves of ground and space observations for 0.25 day coverage of SZ Lyn. The phases are synchronized at the peaks and hence the WASP and APT data do not start at 0. The power spectra in the frequency range 2 - 50 c/d is shown in the right panel corresponding to each data source. V band light curves are shown for the Mount Abu and APT data. The amplitude of the light curves are in magnitude scale where the ground based data is differential and TESS fluxes are converted to magnitudes.

based observations were highly unevenly sampled and LS is specially designed to pick out periodic variations in such kind of data. The LS periodogram tool is available in the VARTOOLS software package (Hartman 2012). The highest frequency to search is the Nyquist frequency ($f_{\rm Nq}$) and should be derived from the data set. For TESS data this is approximately 360 c/d. $f_{\rm Nq}$ of the ground based observations differ due to the uneven observation parameters. Although the higher sampling rate of ground observations would result in a higher $f_{\rm Nq}$, their much shorter observation span reduces the upper limit of the searching frequency to much less than 360 c/d. Furthermore, the upper limit of the frequency, 360 c/d, in TESS data cannot be achieved as the S/N ratio drastically decrease at higher frequencies. Therefore, we limit our search to the range 0 - 120 c/d where the frequency peaks are well above the the S/N ratio, with 4σ significant criteria (Breger et al. 1993) for both space and ground based data. In LS analysis, the frequency step size is depending on 1/T, where T is the time span of the observation. The parameter 1/T in frequency analysis is termed as Rayleigh criterion (Aerts et al. 2010). When T is higher the peaks of the power spectrum are narrower. Though the

ground based observation spreads over long range of time, the desired narrowness could not be achieved due to the low duty cycle. This drastic difference in ground and space based power spectra is clearly seen in Fig. 1. Due to the different T in the four data sources, the sampling frequency of LS analysis are different but we ensured that the sampling frequencies were kept more than the highest frequency we expected to find. The light curves were whitened at each peak and applied 5σ clipping in the calculation of the average and RMS of the power spectrum when computing the SNR value of a peak. The power in LS periodogram is normalized to unity (Zechmeister & Kürster 2009) so that the frequency peaks of the four data sources can be compared graphically. Due to the unavailability of phase information of frequencies in LS analysis, we performed the Discrete Fourier Transformation (DFT) using Period04 (Lenz & Breger 2004) keeping the same searching parameters as in LS method and obtained amplitudes and phases of the frequencies. The power spectra for the frequency range of 0 - 100 c/d were obtained by both methods. The frequencies determined by both methods are consistent. Period04 determined the error of the frequencies, amplitudes and phases using 100 iterations of Monte Carlo simulation. Due to the single-site observation, the power spectra of the ground based observations were severely affected by $\pm 1 d^{-1}$ aliasing and its multiples, $\pm 2 d^{-1}$, $\pm 3 d^{-1}$ etc. The power spectra in the range of 0 - 100 c/d for three data sources are shown in Fig. 2. For clarity we exclude the power spectra of WASP data in Fig. 2.

The identified frequencies of both space and ground based observations were tabulated in Table 3. With the long time base observations of TESS, 23 frequencies are identified, while up to 10 of them are discovered in the Mount Abu BVR bands, 8 in the APT UBV bands and 5 in WASP data. Though the frequency extraction from the ground based observations is more complicated due to the low observation span and gaps, we used pre-whitening and the *killharm* routine in VARTOOLS to carefully remove the fundamental frequency of f_1 8.296 c/d and its first three harmonics (corresponding to frequencies of 16.590, 24.890 and 33.187 c/d), as well as the $\pm 1 d^{-1}$ day aliasing. The first four frequencies were removed from the Mount Abu data using their fourier components and the residual light curve was obtained. The residuals were again subjected to LS and DFT. The rest of the multiples ($5\times f_1$ to $8\times f_1$) of ground based data were found using these residual light curves. Eight common frequencies were clearly identified in Mount Abu and APT power spectra while WASP detected only up to four frequencies. The main pulsation frequency f_1 of 8.296 c/d and its seven harmonics were common in space and ground. In addition, there are six more harmonics of f_1 present in TESS data. The harmonics above f_3 are newly discovered for SZ Lyn in this work. The f_1 of 8.296 c/d, that we identify as the fundamental radial mode, had previously been identified by Gazeas et al. (2004) and is further confirmed by the asteroseismic technique of amplitude ratio method in the Sec. 4.

3.1 New frequencies of SZ Lyn

Most importantly, the frequencies f_2 (14.535 c/d), f_3 (32.620 c/d) and f_4 (4.584 c/d), none of them harmonics of f_1, are new for SZ Lyn. The truncated frequency spectrum in Fig. 3 shows the linear combinations present due to the frequencies f_1, f_2, f_3 and f_4. These linear combinations in one way support that the newly discovered frequencies, f_2, f_3 and f_4, are independent modes. On the other hand, it is possible these are combinations resulted from higher order l modes present in SZ Lyn which cannot be detected due to geometric cancellation. However, the high resolution frequency spectrum from 0 - 120 c/d of TESS does not show any sign of independent frequencies in its higher frequency range so that the possibility of low degree combinations resulting from higher degree modes is minimum. Therefore, we further analyze f_2, f_3 and f_4 assuming they are base frequencies. Fig. 3 shows the combinations made by f_2, f_3 with the well defined radial fundamental frequency f_1. In fact, radial overtones are common in δ Scuti stars, and so we could consider f_2 as an overtone of fundamental. Nevertheless, we estimated the first and second overtones for the well defined period ratios of [0.772 - 0.776] range of Suárez et al. (2006) and [0.611 - 0.632] range of Stellingwerf (1979), respectively. Given that the fundamental radial mode is 8.296 c/d, the calculated first and second overtones are 10.746 and 13.578 c/d which are not found in the observed power spectra and f_2 is too far from these two overtones as well. Therefore, it is possible to conclude f_2 is a non - radial mode. To determine the spherical degree, l of the non - radial mode, rotational splitting is widely used (Kurtz et al. 2014), (Breger et al. 2011). We noticed that there is an incomplete frequency multiplets around f_2, one at 14.503 and the other 14.435 c/d. Assuming this can be a product of rotational modulation and in order to confirm, we fitted the 14.503 and 14.435 c/d and pre-whitened. The residuals still show several peaks which often occur when a signal changes its amplitude and frequency slightly during the course of the observations. Fourier decomposition of such a signal produces peaks that are not real, but resemble rotational splitting. Another point supporting in this direction is that the f_2 has combination with the main pulsation, f_1, at 22.830 c/d also shows similar asymmetry. This is another clue, although not unambiguous, that we see the beating of a time-variable pulsation signal with the main radial mode.

The frequency f_4 is located in the low frequency range and less than the assumed fundamental radial mode of f_1. Kurtz et al. (2014), Aerts et al. (2010), Breger et al. (1999) strongly state that gravity modes (g-modes) are located in the range 0 - 5 c/d. Therefore, the frequency f_4 could be a medium order gravity mode. Based on the observations of Kurtz et al. (2015), Kurtz et al. (2014), f_4 could be a combination of higher order p-modes or very low order g-modes. The frequency spectrum of SZ Lyn is not crowded with lots of complex combinations in higher frequency region as well as lower side close to zero so that the possibility of f_4 being a combination is very low. Furthermore, Kurtz et al. (2014) shows that the availability of combinations $\nu_1 \pm \nu_g$ with ν_1 and ν_g being the frequencies of the highest amplitude singlet p-mode and a g-mode respectively. These combinations of frequencies produced by fundamental radial p-mode and a g-mode can be naturally explained by non-linear effects that occur when the p-mode and the g-modes are excited simultaneously. The fact that the g-mode frequency distributions are precisely reproduced in both sides of fundamental p-mode is fully consistent with this interpretation of having the combinations of f_1+f_4 (12.880 c/d) and f_1-f_4 (3.703 c/d) in Fig. 3. The availability of these combinations in SZ Lyn

supports the idea that f_4 is a gravity mode excitation and indicates that both p-modes and g-modes are present in SZ Lyn.

Due to the low S/N ratio and also to the possibility of a merging artifact in the vicinity of strong harmonics, ground based power spectra could not clearly detect these three frequencies, f_2, f_3 and f_4. However, the power spectra of Mount Abu were able to just resolve f_2 peak despite the crowded noisy field (See Fig. 2). But the amplitudes of f_2 determined in BVR colour bands of ground based data are highly unreliable; therefore, we could not include f_2 in Sec. 4 to determine the spherical degree l using amplitude ratio method. In order to check the closeness of f_2 for a radial overtone, the pulsation constant, Q was calculated for f_2 and discussed in Sec. 5.2. The amplitudes A and the phases ϕ of the frequency f_1 determined for UBVR colour bands using Period04 are shown in Table 3.

4 AMPLITUDE RATIOS

It is possible to determine the spherical degree l using the amplitude ratios and phase differences in different wavelength bands (e.g., Balona & Evers 1999; Aerts et al. 2010). The process is model-dependent because the amplitude and phase variations not only depend on the spherical harmonic degree l (Balona & Evers 1999), but also –to a lesser extent– on the effective temperatures and gravities of the models as shown in Dupret et al. (2003). In general, flux changes in pulsating stars originate from the temperature and gravity variations as a function of radius (Garrido et al. 1990). The mode identification needs to be done through a sequence of theoretical modeling of different combinations of parameters of the star. Theoretical aspects of flux change of the model star were discussed in detail with the consideration of non-adiabatic parameters and limb darkening effect by Watson (1988) and Heynderickx (1994).

The spherical degree can be identified by matching the observed amplitude ratios with the theoretically predicted amplitude ratios for the different stellar model atmospheres. The magnitude variation of a pulsating star, Δm_λ, at wavelength λ with a spherical harmonic degree l at a pulsating frequency ω can be expressed as:

$$\Delta m_\lambda = A_0 P_{lm}(\cos\ i) b_{l\lambda}(T_1 + T_2 + T_3) e^{i\omega t} \quad (1)$$

$$T_1 = (1-l)(l+2)$$
$$T_2 = f_T(\alpha_{T\lambda} + \beta_{T\lambda}) e^{-i\psi_T}$$
$$T_3 = -f_g(\alpha_{g\lambda} + \beta_{g\lambda})$$

where P_{lm} is the associated Legendre function of degree l and azimuthal number m, A_0 is related to the amplitude of oscillations of the photosphere, and i is the inclination angle between the stellar axis and the direction towards the observer. For the derivation and the details of the components in Eq. 1, refer to Watson (1988), Heynderickx (1994), Balona & Evers (1999) and Dupret et al. (2003). The component T_1 is the contribution of the magnitude variation due to the different pulsation modes. T_2 is the temperature dependent component of the magnitude which consists of f_T, the amplitude of temperature variation function relative to the normalized radial displacement at the photosphere and ψ_T, the phase difference between maximum temperature and maximum radial displacement. T_3 represents gravity variation where f_g is the amplitude of gravity variation function to the normalized radial displacement at the photosphere (Dupret et al. 2003). The determination of f_T is highly dependent on the non-adiabatic parameter R (Garrido 2000a). The other two parameters, ψ_T and f_g are also unknown for any stellar model. The method of mode identification therefore depends on the correct combination of these parameters which were done earlier by different techniques, approximating the observations to the theoretical models for reasonable ranges of f_T and ψ_T (Balona & Evers 1999). The value of R was estimated by Heynderickx (1994) by adjusting it for best fit of the observed light curves, while Garrido et al. (1990) redefined it as a range of interest keeping R and ψ_T as free parameters in the range [0.25 − 1] and [90° − 135°] respectively for δ Scuti stars. Dupret et al. (2003) improved the non-adiabatic treatment of the model atmosphere and proposed a method of determination of amplitudes f_T, f_g of the eigenfunctions and the phase ψ_T for different degree l for a range of effective temperatures $T_{\rm eff}$, $\log(g)$ and mass of the star. In this work, we used the outputs of non-adiabatic computations provided by M. A. Dupret (private communication) for SZ Lyn. The input parameters $T_{\rm eff}$=7540 K, $\log(g)$=3.88 (Langford 1976) and M=1.57 $M_\odot$ (Fernley et al. 1984) were passed to the non-adiabatic code to generate the pulsation models which give frequencies close to the observed main frequency of 8.296 c/d. The two resulting-models that are close to our observational results are shown in Table 5. The output of the non-adiabatic code also provides the amplitudes of f_T, f_g and phase angle ψ_T for frequencies for different degree. Fitting polynomials for different degree, l, as shown in Fig. 6 determined f_T, f_g and ψ_T for the observed frequency f_1. We have shown only the $l = 0$ mode in Fig. 6 for the present purpose.

For the partial derivatives of the monochromatic flux, $\alpha_{T\lambda}$ and $\alpha_{g\lambda}$ (Eq. 1), we used ATLAS9 model atmospheres and fluxes by Kurucz (1993), Castelli (2003). Due to the complexity of lookup tables in all UBVR bands of Kurucz grid for the computation of $\alpha_{T\lambda}$ and $\alpha_{g\lambda}$, we produced a code, AlphaTg, to readout the model fluxes from the grid for the desired range of temperature and $\log(g)$ with a step size of 250 K and 0.5 respectively. The partial derivatives, $\alpha_{T\lambda}$ and $\alpha_{g\lambda}$ computed within the observational error box of SZ Lyn using AlphaTg code are shown in Fig. 4. It is clear that the temperature contribution ($\alpha_{T\lambda}$) to the magnitude variation and hence to the theoretical amplitudes is much more effective than the gravity component ($\alpha_{g\lambda}$), as seen in Fig. 4. Since the non-adiabatic parameters of f_T, f_g and ψ_T were computed for the solar metallicity of $Z = 0.014$, we used the solar metal abundance of $[M/H] = 0.0$ model from the Kurucz grid for the partial derivatives in the range of desired temperature and $\log(g)$. All the flux models were computed with the turbulence velocity fixed at 2 km/s and a mixing length parameter (α) of 1.25. The non-adiabatic models in Table 5 did use a metal abundance of $Z = 0.014$ which is in good agreement with the metal abundance of model atmospheres. Furthermore, Garrido (2000a) has shown that the flux derivatives have no significant change with the metallicity except in blue band. The variation of flux derivatives in Fig. 4 also provides similar results as the relative variation is

Table 3. Frequencies and amplitudes of SZ Lyn. V band data only are shown for Mount Abu and APT. The amplitude is in Lomb-Scargle Power (LSP).

ID	TESS Frequency (c/d)	TESS Amplitude (LSP)	Mount Abu Frequency (c/d)	Mount Abu Amplitude (LSP)	APT Frequency (c/d)	APT Amplitude (LSP)	WASP Frequency (c/d)	WASP Amplitude (LSP)
f_1	8.296	0.8496	8.296	0.8269	8.296	0.8668	8.296	0.6795
$2f_1$	16.592	0.8321	16.590	0.5332	16.592	0.8330	16.593	0.2606
$3f_1$	24.889	0.7724	24.890	0.1647	24.889	0.7148	24.890	0.0658
$4f_1$	33.186	0.5874	33.186	0.0330	33.185	0.4110	33.185	0.0264
$5f_1$	41.482	0.3709	41.483	0.0170	41.481	0.2099	41.567	0.0101
$6f_1$	49.779	0.2205	49.849	0.0058	49.777	0.1444		
$7f_1$	58.075	0.0680	58.065	0.0040	58.157	0.0397		
$8f_1$	66.372	0.0478	66.365	0.0017	66.339	0.0273		
f_2	14.535	0.0376	14.016	0.0162				
$9f_1$	74.668	0.0153	73.120	0.0055				
$f_2 + f_1$	22.830	0.0069						
f_3	32.620	0.0062						
$10f_1$	82.965	0.0054						
$f_2 - f_1$	6.237	0.0040						
$f_3 + f_1$	40.888	0.0018						
f_4	4.584	0.0013						
$f_1 - f_4$	3.703	0.0011						
$f_3 - f_1$	24.308	0.0015						
$11f_1$	91.261	0.0015						
$12f_1$	99.564	0.0007						
$f_1 + f_4$	12.880	0.0006						
$13f_1$	107.824							
$14f_1$	116.104							

Table 4. Observed amplitudes (A in magnitude) and phases (ϕ in radians) for the main frequency f_1=8.296 c/d obtained from PERIOD04. Only f_1 is included in the table as this is the only independent frequency available in multi-band photometry of ground based data. The observed amplitude ratios in the middle row were used in Sec. 4. The last row is phase differences in degrees. The phase zero is at 2457480.63391813 HJD.

	U	B	V	R
A	0.275±0.003	0.290±0.004	0.229±0.003	0.171±0.002
ϕ	0.834±0.003	0.805±0.003	0.803±0.003	
	A_U/A_B	A_B/A_B	A_V/A_B	A_R/A_B
	0.95±0.02	1.00	0.79±0.02	0.59±0.02
	$\phi_U - \phi_B$	$\phi_U - \phi_V$		
	1.7±0.2	1.8±0.2		

Table 5. Best-fitting theoretical models of SZ Lyn

Model 1		
$M/M_\odot$=2.00	$T_{\rm eff}$=7522 K	$\log(L/L_\odot)$=1.425
$\log(g)$=3.77	$R/R_\odot$ = 3.00	age(yr)=1.0×10^9
X=0.72	Z=0.014	α = 1.7
Model 2		
$M/M_\odot$=1.90	$T_{\rm eff}$=7557 K	$\log(L/L_\odot)$=1.322
$\log(g)$=3.86	$R/R_\odot$ = 2.68	age(yr)=1.1×10^9
X=0.72	Z=0.014	α = 1.7

much higher for shorter wavelengths. Balona & Evers (1999) pointed out that amplitude discrimination is more effective in shorter wavelength bands because of this variation in flux derivatives. Breger et al. (1998) showed the mixing length parameter, α, is in between 1 and 2 for δ Scuti stars and less effective on hot stars. Therefore, mixing length parameter α was set to 1.25 which is one of the two options available in the ATLAS9 models for the calculations of flux derivatives.

Limb darkening effect was added to the theoretical amplitude by computing limb darkening integral using the simple linear limb darkening law given by Claret & Hauschildt (2003) in Eq. 2.

$$b_{l\lambda} = \int_0^1 \mu I(\mu) P_l d\mu \qquad (2)$$

$\frac{I(\mu)}{I(1)} = 1 - u(1-\mu)$
where u is the limb darkening coefficient.

The AlphaTg code was used with linear model in Eq. 2 for the computation of limb darkening integrals and hence obtained the partial derivatives of $\beta_{T\lambda}$ and $\beta_{g\lambda}$ shown in Fig. 5. The limb darkening integral $b_{l\lambda}$ depends on the mode of the oscillation l. From the grids of limb darkening coefficients provided by Claret & Hauschildt (2003), the limb darkening integrals were computed for UBVR bands and hence obtained derivatives, $\beta_{T\lambda}$ and $\beta_{g\lambda}$, for three spherical degrees of l (l=0,1,2) in the range of effective temperatures and gravity of the two proposed models of SZ Lyn. The results are shown in Fig. 5. The limb darkening derivatives of temperature in upper panel of Fig. 5 are more sensitive to $l = 0$

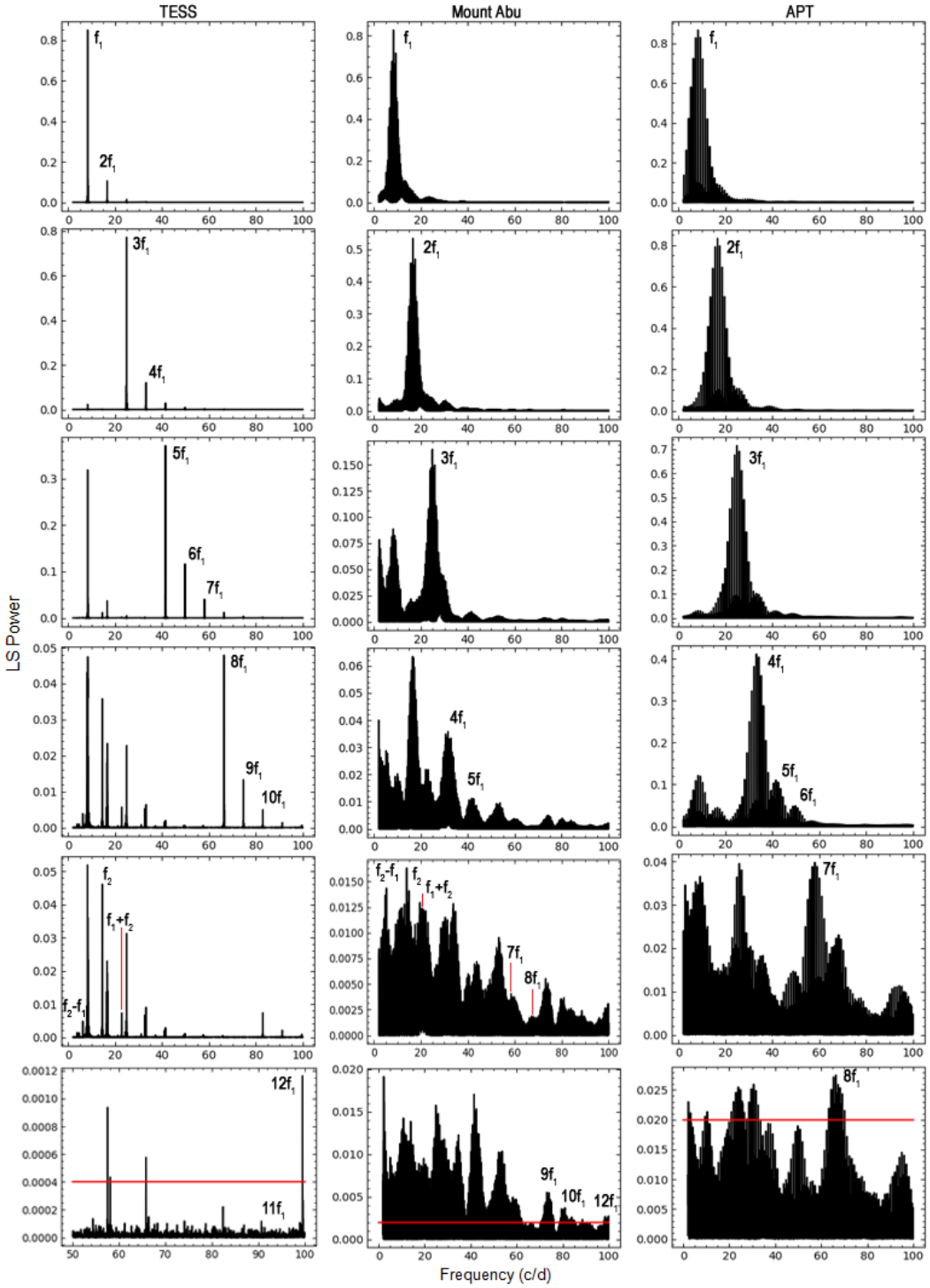

Figure 2. The comparison of LS power spectra of space and ground base observation. The low amplitude frequencies were recovered by whitening the previously determined frequencies f_1, $2f_1$, $3f_1$ etc. The horizontal red line in the last row indicates the 4σ threshold line for cut off.

degree as well as for lower wavelengths while derivatives are less effective for $l = 2$. Besides, the gravity counterpart of limb darkening derivative (lower panel, Fig. 5) compared to the temperature is very much less particularly in the range of $log(g)$ of SZ Lyn. The effect of gravity change is less effective for mode discrimination than that of temperature, suggesting that the effect of gravity on limb darkening is negligible compared to the effect of temperature. This effect is previously shown by Garrido (2000a). This was clearly pointed out by Dupret et al. (2003) introducing the non-adiabatic treatment, the dimensionless frequency K is smaller for low order p-mode so that the difference between f_T and f_g is smaller and hence the impact of variation in gravity is minimum. However, we consider limb darkening integrals due to

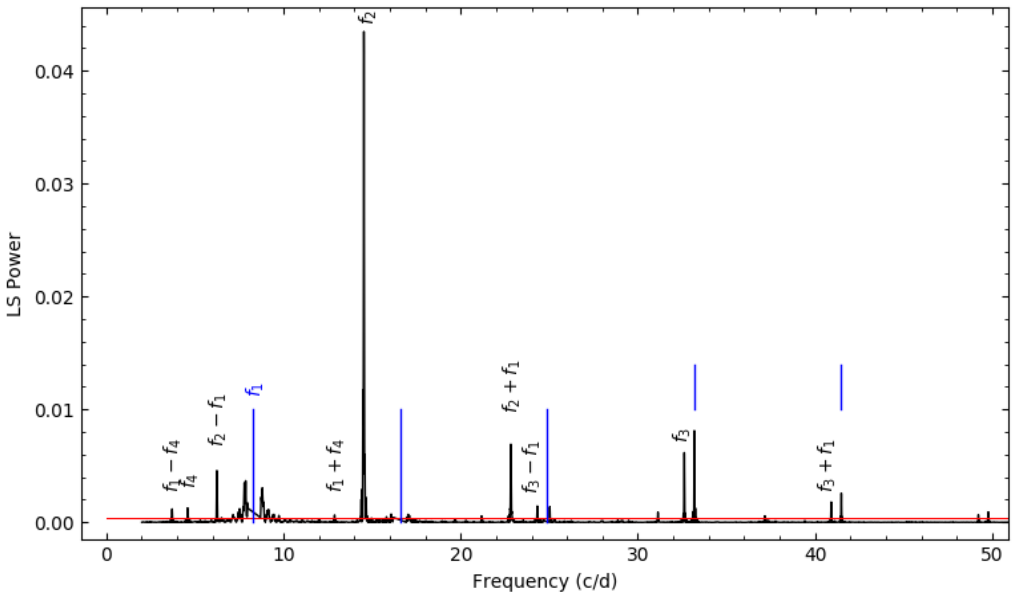

Figure 3. New set of frequencies and their combinations with the fundamental frequency f_1 detected in SZ Lyn using TESS data. The blue lines indicate the location of the whitened frequencies of f_1 and the first four harmonics. The discontinuity at the frequency f_1 is due to the removal of strong side-lobes created by f_1. The horizontal red line is the 4σ threshold line for cut off.

gravity, even though negligible, in our calculations of theoretical amplitudes because of the model parameters of SZ Lyn in Table 5 are very close to each other. The theoretical amplitude ratios of l= 0, 1 and 2 calculated for Model 1 and Model 2 in Table 5 and observed amplitude ratios taken from Table 4 for frequency f_1 are compared in Fig. 7 and Fig. 8. Since observations are scattered and the two model parameters are very close to each other, in order to better assess the appropriateness of the different values for l as well as to converge for the best model, we computed the χ^2 function in Eq. 3 for different degree l which is shown in Fig. 9

$$\chi^2(l) = \sum_{j=1}^{\text{filters}} \left(\frac{A_{j,\text{th}}/A_{\text{ref,th}} - A_{j,\text{obs}}/A_{\text{ref,obs}}}{\sigma_{j,\text{obs}}} \right) \quad (3)$$

The χ^2 minimization resulted in the conclusion that the frequency f_1 is better fitted to $l = 0$ degree of Model 2 and therefore Model 2 is more appropriate to represent the physical properties of SZ Lyn.

5 PHYSICAL PARAMETERS OF SZ LYN

We try to redefine the physical parameters of SZ lyn in this asteroseismic investigation of SZ Lyn. Although the fundamental radial mode, f_1, is clearly defined in early literature, we fit two modes of SZ Lyn using amplitude ratio method in Sec. 4 not only confirming f_1 is a radial fundamental mode but also finding that the physical parameters of SZ Lyn are close to Model 2. However, these two models parameters are very close to each other resulting the difference of the minimum χ^2 of the two models for $l = 0$ is about 3 (See Fig. 9). Therefore, we look at other possibilities to confirm which model is more appropriate for SZ Lyn.

5.1 Evolutionary status of SZ Lyn

The physical parameters of the star can be refined by using observations to constrain the appropriate stellar models. We have computed evolutionary sequences using version 11701 of the MESA stellar evolution code (Paxton et al. 2011, 2013, 2015, 2018, 2019) for stars with masses ranging from 1.80 $M_\odot$ to 2.0 $M_\odot$ in steps of 0.05 $M_\odot$. The evolutionary models were computed for the standard solar composition of $Z = 0.014$ (Asplund et al. (2009), hereinafter AGSS09). In all the computed sequences the opacities are from OPAL (Rogers & Iglesias 1996). The models have been computed using mixing length parameter α=1.25 or 1.7 and overshooting of $0.2H_P$ at all convective boundaries. The sequences for these two values of the mixing-length parameter are very close, and then have no impact on our analysis for the likely physical parameters of SZ Lyn. The nuclear network is *pp_and_cno_extras.net*, that includes 25 isotopes ranging from ^{1}H to ^{24}Mg. We have not considered mass-loss nor rotation for the evolutionary sequences.

Fig. 10 shows the HR diagram of the evolutionary models computed with $\alpha = 1.25$ and using the AGSS09 chemical composition. Model 1 and 2 both placed reasonably well in the standard position of δ Scuti stars in the evolutionary models (Pamyatnykh 1999). Both models can be beyond the Termination Age Main Sequence (TAMS) for evolutionary sequences with M=1.80$M_\odot$ and 1.90$M_\odot$ or, in the case of the Model 2, could be passing the Main Sequence (MS) for models with M=1.85$M_\odot$ or M=1.90$M_\odot$. Clearly, the evolu-

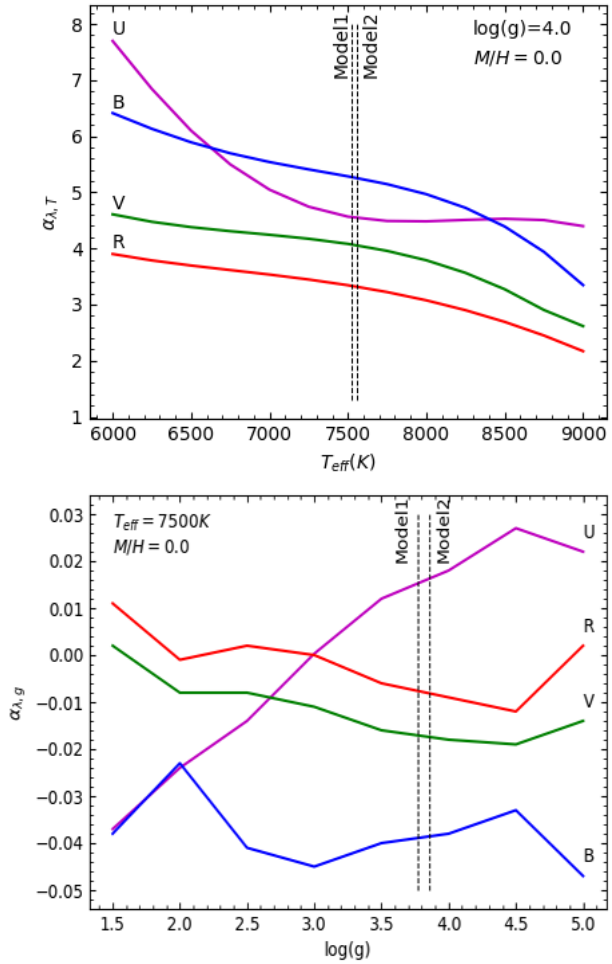

Figure 4. Flux derivative as a function of temperature (upper panel) and as a function of gravity (lower panel) generated by AlphaTg code. The two dashed line indicates the two models proposed for SZ Lyn in Table 5. The derivatives taken at these two models were used for the calculation of theoretical amplitudes.

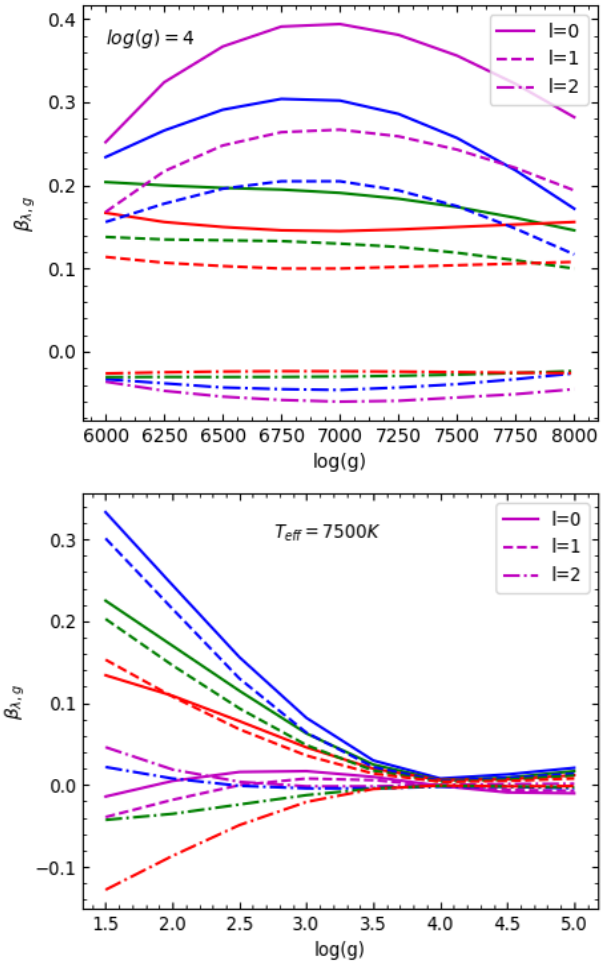

Figure 5. Limb darkening derivatives. The upper panel shows the variation of limb darkening derivative with temperature for all three modes of l and for UBVR colour bands for $\log(g) = 4$. The colours, Violet, Blue, Green and Red represent the UBVR bands respectively. Lower panel shows limb darkening derivatives with gravity for l and UBVR for $T_{\rm eff}$ = 7500 K.

tionary sequences show that SZ Lyn might have a mass in the range 1.80–1.90 $M_\odot$, but we can not decide from the tracks which is the correct value.

5.2 Pulsation constant

The pulsation constant (Q) can be determined for the frequency f_1 using the Eq. 4 given by Breger (1990) for the two models mentioned in Table 5.

$$\log(Q) = \log(P) + \frac{1}{2}\log(g) + \frac{1}{10} M_{\rm bol} + \log(T_{\rm eff}) - 6.454 \quad (4)$$

The bolometric magnitude $M_{\rm bol}$ of SZ Lyn is estimated for two models using the values found in Table 5. We take for the solar bolometric absolute magnitude the standard value of $M_{\odot{\rm bol}}$=4.74 (Bessell et al. 1998; Torres 2010) and solar luminosity $L_\odot = 3.85 \times 10^{33}$ erg s^{-1}. The pulsation constant Q is then found to be 0.032 for Model 1 and 0.038 for Model 2. The stellar parallax of SZ Lyn obtained by *Gaia* mission provides an absolute magnitude M_V of +1.14. and the bolometric correction (BC) is -0.094 as given by Cox (2000), thus resulting in a bolometric absolute magnitude for SZ Lyn of $M_{\rm bol}$ +1.05. This results in an alternative set of Q values of 0.031 and 0.035 for Model 1 and Model 2 respectively. The pulsation constant for fundamental radial p-modes in δ Scuti stars is in the range of $0.022 \leq Q \leq 0.033$ (Breger 1975) and an even narrower range of $0.0327 \leq Q \leq 0.0332$ fundamental radial mode pulsation (Fitch 1981). The calculations show that the Q value for Model 1 is within the allowed range given by Breger (1975) and close to the lower limit of the range given by Fitch (1981), and this gives us confidence that the frequency f_1 is the radial fundamental mode of stellar pulsation. On the other hand, the Q value of radial fundamental mode of Model 2 parameters is slightly deviated from the standard intervals.

The frequency f_2 was identified as non-radial mode in the frequency analysis based on the period ratio method given that f_1 as the fundamental radial mode. We checked the pulsation constant, Q, assuming the frequency f_2 as a radial overtone. The stellar parameters of Model 1 and Model 2 were passed to the Eq. 4 with the corresponding period of

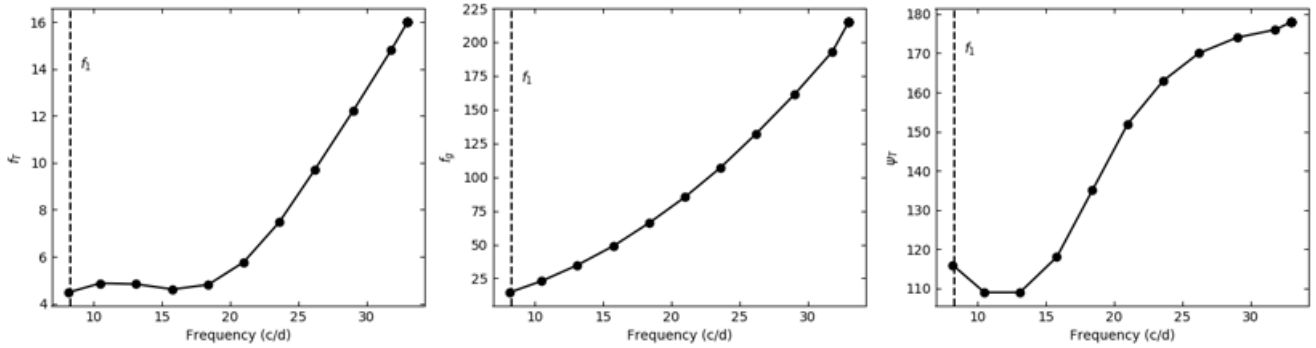

Figure 6. f_T, ψ_T and f_g as a function of the pulsation frequency (c/d) for the mode of degree l=0 for Model 1. The dashed line indicates the observed frequency f_1. Since f_2, f_3 and f_4 are not identified in multi-band observation these three frequencies are not included.

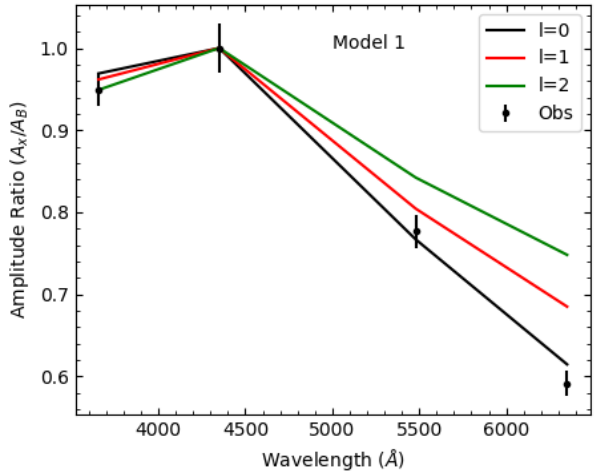

Figure 7. The observed amplitude ratios and the computed amplitude ratios for the Model 1 for the frequency f_1. Dots with error bars are the observed amplitude ratios and the lines are the theoretical predictions for degree, l.

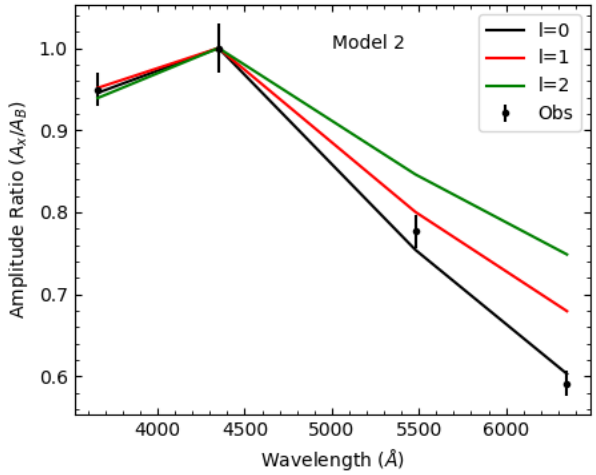

Figure 8. The observed amplitude ratios and the computed amplitude ratios for the Model 2 for the frequency f_1.

f_2 and obtained Q=0.018 and Q=0.022 respectively. Fitch (1981) modeled the pulsation constants of 1st and 2nd harmonics as 0.025 and 0.020 for δ Scuti stars of 2M$_\odot$. Although the pulsation constant of f_2 with the Model 2 parameters is close to the 2nd harmonic, Breger (2000b) pointed out that the calculation of Q values from photometric parameters is subjected to systematic errors as large as $\approx$ 25%. Therefore, we could not specifically say even the pulsation constant of f_2 is 0.022 for Model 2, nor whether the frequency f_2 is an overtone of fundamental.

5.3 HELAS model oscillations

Furthermore, we considered HELAS oscillation models to confirm the parameters of SZ Lyn. The pulsation models produced by using OPAL opacities Rogers & Iglesias (1996) and AGSS09 chemical composition Asplund et al. (2009) from ZAMS to TAMS for radial and non-radial oscillations were searched in the HELAS[3] set of models. In this database, three pulsation models of masses M=1.8 M$_\odot$, M=2.0 M$_\odot$ and M=2.2 M$_\odot$ were found with the oscillation frequency close to f_1, 8.296 c/d, of radial mode. The frequency distribution of radial (l=0) and non-radial (l=1, l=2) pulsations with the physical parameters for the three models are shown in Fig. 11. The model of mass M=2.0 M$_\odot$ has a radial fundamental frequency which is closest to the observed fundamental radial mode of f_1. The other two frequencies, f_2, f_3 are also overlapping with the model frequencies of l=2 mode of the same model of mass M=2.0 M$_\odot$. Therefore, our judgement of non-radial mode of f_2 and f_3 in both frequency analysis and pulsation constant strengthen by these models of having non-radial modes close to the observed f_2 and f_3. Although it is not sufficient for a solid conclusion of the spherical degree of f_2 and f_3 as l=2 but can be conclude they likely are non-radial modes. Through this convergence of the HELAS's three models, the physical parameters of M=2.0 M$_\odot$ pulsation model is in line with Model 1 in Table

[3] http://helas.astro.uni.wroc.pl/deliverables.php?active=opalmodel&lang=en

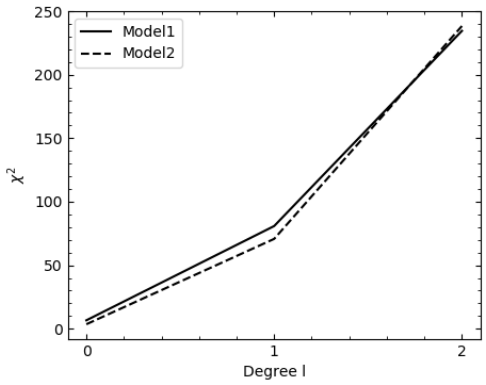

Figure 9. Chi square minimization of frequency f_1 to the degree l for the Model 1 and Model 2.

5, except for the low effective temperature of 7396 K. The radial fundamental frequencies of the models, M=1.8 $M_\odot$ and M=2.2 $M_\odot$, are far from the observed f_1 and also does not support to have f_2 and f_3. Neither the physical parameters of M=1.8 $M_\odot$ and M=2.2 $M_\odot$ are close to our Model 1. Therefore, HELAS models also provide evidence a star of mass M≈2.0 $M_\odot$ which oscillates in radial fundamental mode of 8.296 c/d as well as having some non-radial modes close to the observed frequencies.

Hence, considering all the results of this section, we infer that the mass of SZ Lyn should be within $1.8M_\odot<M<2.0M_\odot$.

5.4 Mean density

As we have only determined a single radial mode without any strongly confirmed overtones, we cannot use the period ratios to determine the average density of the star. Nevertheless, we could estimate the average density of SZ Lyn using the Q values, calculated in Sec. 5.2, using the relation:

$$P = Q(\rho/\rho_\odot)^{-1/2} \quad (5)$$

where P is the period of the fundamental oscillation in days and Q is the pulsation constant. The average density of the Sun is $\rho_\odot$= 1.4103 g cm^{-3} and our stellar pulsation models in Sec. 4 predicted the Q values of 0.035 for the Model 2 result in an average density of ρ=0.1189 gcm^{-3}.

Furthermore, with the fundamental period of SZ Lyn, P = 0.1205299 d and for more narrow range of Q values $0.0327 \leq Q \leq 0.0332$ (Fitch 1981), we find the average density $\rho = 0.1054 \pm 0.0016$ gcm^{-3}. Suárez et al. (2014) computed the mean densities of δ Scuti stars using their virtual observatory tool, TOUCAN, found that the fundamental frequency range of 95 - 113 μHz (0.121832 - 0.102425 d) has relative densities ($\rho/\rho_\odot$) less than 0.11. Hence we can conclude that the density of $\rho = 0.1054 \pm 0.0016$ gcm^{-3} is an appropriate value for SZ Lyn.

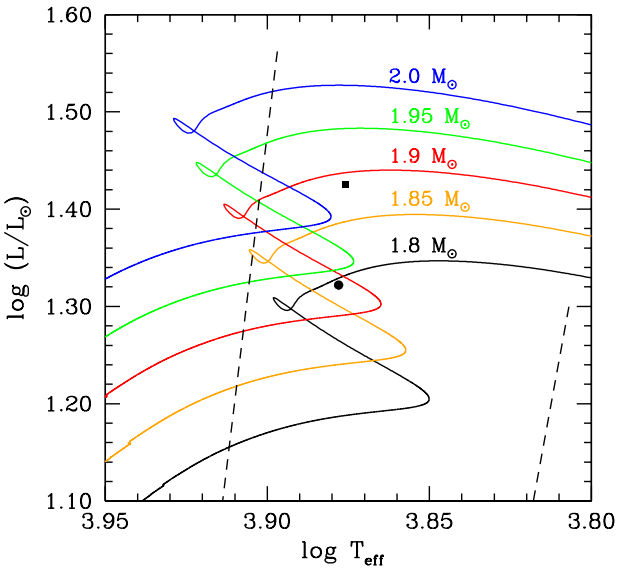

Figure 10. Main and post-main sequence evolutionary tracks of stars in the range 1.8–2.0 $M_\odot$ for an AGSS09 chemical composition (Z=0.014) for $\alpha = 1.25$; the tracks for $\alpha = 1.7$ are very close to the ones shown in the figure and have not been included. The two models in Table 5 are shown as a square (Model 1) and a circle (Model 2). Dashed lines show the limits of the instability strip

6 DISCUSSION

SZ Lyn has been extensively studied by several authors who have analysed their results considering both its binary nature as well as its pulsating nature. Though its binary orbital characteristics have been studied in detail, the comprehensive asteroseismic studies of SZ Lyn are few. We reconsider SZ Lyn giving special attention to recovering more frequencies apart from the main frequency, and determining the degree of the oscillation. With this information, we have tried to refine its stellar parameters.

We confirmed 23 frequencies, 14 of which are multiples of the fundamental frequency f_1. Gazeas et al. (2004) also confirmed the frequency f_1 and its first two harmonics, and we discovered 11 new harmonics in SZ Lyn. Therefore to confirm the radial mode, we adopted the amplitude ratio method as it provides a consistent result with the observed amplitudes. In addition to the amplitudes, δ Scuti stars show wavelength dependence on the phase. A method proposed by Garrido et al. (1990) showed that mode can be determined by plotting amplitude ratio versus phase difference for two colors. This method was performed for Strömgren photometric system taking two bands each time and plotting the so-called area of interest for a broad range of parameters of ψ_T and non-adiabaticity R. Although the phase difference

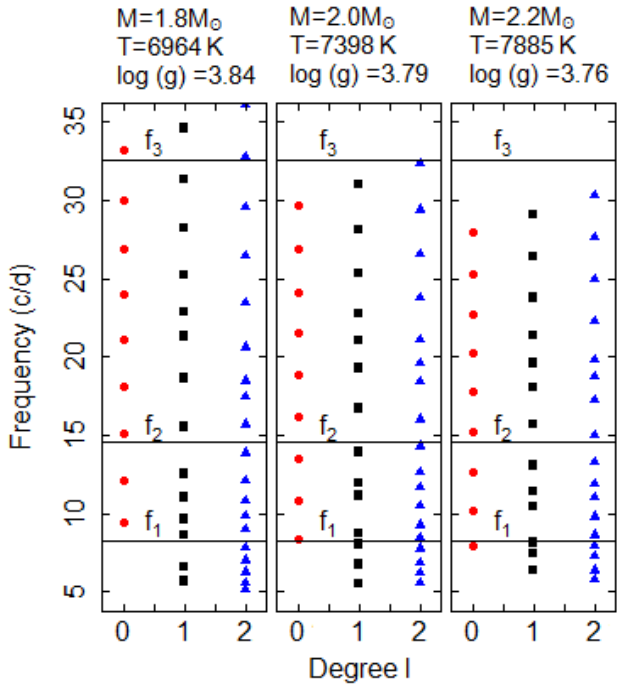

Figure 11. Radial and non-radial frequencies of HELAS pulsation models of masses M=1.8M$_\odot$, M=2.0M$_\odot$ and M=2.2M$_\odot$. V$_{\rm rot}$=0. Red, Black and Blue symbols represent l=0, l=1 and l=2 respectively. The horizontal lines represent the observed frequencies of SZ Lyn. The error bars of the observed frequencies are too small to visualise. 0 - 5 c/d range is omitted for clarity.

method is more appropriate for δ Scuti stars to determine the degree of the modes, we did not represent it graphically because of the availability of one frequency (f_1) in multi-band photometry and there are no other frequencies to compare. But the phase difference of the frequency f_1 shown in Table 4, $\phi_{\rm U} - \phi_{\rm B}$ and $\phi_{\rm U} - \phi_{\rm V}$ both are greater than zero (Breger 2000a; Garrido 2000b), thus further confirming that f$_1$ corresponds to a radial mode of l=0. Furthermore, the TESS observations clearly revealed the presence of independent frequencies f_2=14.535 c/d, f_3=32.620 c/d and f_4=4.584 c/d. Unfortunately these frequencies do not recover in the multi-band ground based data, therefore, we could not perform the amplitude ratio method to determine the spherical degree l. However we were able to conclude that f_2 and f_3 are non-radial modes through the period ratio method and pulsation constant calculations. In addition, the HELAS pulsation models give some evidences that f_2 and f_3 are close to l=2 mode but we refrain from confirming the mode of f_2 and f_3 as further investigations are needed. The discovery of frequency f_4 is remarkable because it is identified as medium-order g-mode pulsation which is rare in δ Scuti stars.

As a consequence of the determination of independent frequencies and their modes, this investigation is used to refine the stellar parameters of SZ Lyn. In the process of determining the degree of the mode l of the frequency f_1 using amplitude ratio method, it is possible to compare SZ Lyn to an appropriate set of evolution sequences with different stellar parameters. With the availability of global parameters of SZ Lyn which were determined earlier, we searched the best model for SZ Lyn out of two models. We explored parameters of the model, basically T$_{\rm eff}$ ($\pm 250K$) and log(g) ($\pm$0.5). Although the flux and limb darkening derivatives are available for any T$_{\rm eff}$ and log(g), the limitation of the eigenvalues, f_T, f_g and ψ_T, computed using a non-adiabatic code restricted the evaluation only for the two valid models detailed in Table 5. The two models, with T$_{\rm eff}$=7522 K, log(g)= 3.77 and $T_{\rm eff}$=7557 K, log(g)=3.86, which do not differ much from each other, were evaluated with the observed fundamental frequency of SZ Lyn by means of different techniques in order to identify the best model. We found that the amplitude ratio method was consistent with Model 2.

Table 6. Physical parameters of SZ Lyn

Physical Property	Value	Remarks
$T_{\rm eff}$	7557 K	This paper
	7540 K	Langford(1976)
	7235 K	LAMOST
	7799 K	*Gaia*
log(g)	3.86	This paper
	3.88	Langford(1976)
	3.94	LAMOST
Mass (M)	1.9$\pm$0.1 M$_\odot$	This Paper
	1.57(+0.17)M$_\odot$	Fernley(1983)
Radius (R)	2.68R$_\odot$	This paper
	2.76R$_\odot$	Fernley(1983)
	2.80R$_\odot$	Bardin(1981)
Mean density (ρ)	0.1054$\pm$0.0016 g cm^{-3}	This paper

The evolutionary sequences of MESA were determined to get a better approximation of the mass of SZ Lyn. The placement of Model 1 and Model 2 in H-R diagram showed slightly differences with the tracks that result in an uncertainty in terms of mass roughly equivalent to $\pm$0.1M$_\odot$. Therefore, we accepted the mass of Model 2, 1.9M$_\odot$ with an error of $\pm$0.1M$_\odot$. This error is in good agreement with HELAS's models which converged to 2M$_\odot$. In addition, the two models were tested using the pulsation constant Q. In this attempt of convergence between theoretical models and observed data, Model 1 is closer to the observations. Furthermore, we compared the parameters of Model 1 and 2 with HELAS pulsation models to see the consistency of our analysis. Within the uncertainties, it is possible to conclude that Model 2 is more appropriate to represent the parameters of SZ Lyn. Finally, the stellar parameters determined through this analysis and the previous observations were tabulated in Table 6.

The uncertainties of the parameters cannot be determined with the help of evolutionary models. Since the determination of parameters sensitively depends on these models, it is reasonable to take the step sizes of the models as the standard error as a rough, first approximation. In such a way the temperature can be deviated by $\pm$35 K.

7 CONCLUSION

The well resolved TESS data recovered 23 frequencies in SZ Lyn. Apart from the fundamental radial mode of 8.296 c/d and its two harmonics, we found 3 independent modes and 10 harmonics of the fundamental frequency. Though the ground based data is not up to the standard of TESS, most of the harmonics and one independent mode are present in the Mount Abu light curve also. The presence of the dominant p-mode of radial fundamental at 8.296 c/d, non-radial p-modes at 14. 535 c/d, 32.620 c/d and a g-mode at 4.584 c/d indicates all possible oscillations can be simultaneously occurred at a same star. Finally, the UBVR ground based observation made important over space based data as the ground based data can be used to approximate a theoretical model to SZ Lyn and hence determine stellar parameters mentioned in Table 6.

ACKNOWLEDGEMENTS

We thank M. A. Dupret for providing non-adiabatic computation results. JA acknowledges the support of the Centre for International Cooperation in Science, Govt. of India for his work and stay at PRL when some of the work presented here was completed. JA's earlier work at PRL was under a UN sponsored CSSTEAP (Centre for Space Science Technology and Education in Asia Pacific) program. We thank the staff at the Mount Abu IR Observatory for their technical support during the course of this work. We are also very grateful to the staff of Arthur C Clarke Institute for their invaluable administrative support. We thank Prof U C Joshi and Prof H O Vats, for their support and useful discussion at various times through this work. SJ acknowledge the discussion with Dr. Dogus Ozuyar on evolutionary part. This work is supported by the Department of Space, Govt. of India. GH gratefully acknowledges funding through NCN grant 2015/18/A/ST9/00578.

"This paper makes use of data from the first public release of the WASP data (Butters et al. 2010) as provided by the WASP consortium and services at the NASA Exoplanet Archive, which is operated by the California Institute of Technology, under contract with the National Aeronautics and Space Administration under the Exoplanet Exploration Program."

Guoshoujing Telescope (the Large Sky Area Multi-Object Fiber Spectroscopic Telescope LAMOST) is a National Major Scientific Project built by the Chinese Academy of Sciences. Funding for the project has been provided by the National Development and Reform Commission. LAMOST is operated and managed by the National Astronomical Observatories, Chinese Academy of Sciences. This work has made use of data from the European Space Agency (ESA) mission *Gaia* (`https://www.cosmos.esa.int/gaia`), processed by the *Gaia* Data Processing and Analysis Consortium (DPAC, `https://www.cosmos.esa.int/web/gaia/dpac/consortium`). Funding for the DPAC has been provided by national institutions, in particular the institutions participating in the *Gaia* Multilateral Agreement.

This paper includes data collected by the TESS mission. Funding for the TESS mission is provided by the NASA Explorer Program. Funding for the TESS Asteroseismic Science Operations Centre is provided by the Danish National Research Foundation (Grant agreement no.: DNRF106), ESA PRODEX (PEA 4000119301) and Stellar Astrophysics Centre (SAC) at Aarhus University. We thank the TESS team and staff and TASC/TASOC for their support of the present work.

REFERENCES

Aerts C., Christensen-Dalsgaard J., Kurtz D. W., 2010, Asteroseismology. Springer
Alania I., 1972, Information Bulletin on Variable Stars, 702
Antoci V., et al., 2019, Monthly Notices of the Royal Astronomical Society, 490, 4040
Asplund M., Grevesse N., Sauval A. J., Scott P., 2009, ARA&A, 47, 481
Balona L., Evers E., 1999, Monthly Notices of the Royal Astronomical Society, 302, 349
Balona L., Holdsworth D. L., Cunha M., 2019, Monthly Notices of the Royal Astronomical Society, 487, 2117
Bardin C., Imbert M., 1981, A&A, 98, 198
Barnes III T. G., Moffett T. J., 1975, The Astronomical Journal, 80, 48
Bessell M. S., Castelli F., Plez B., 1998, A&A, 333, 231
Binnendijk L., 1968, The Astronomical Journal, 73, 29
Bowman D. M., Buysschaert B., Neiner C., Pápics P. I., Oksala M. E., Aerts C., 2018, A&A, 616, A77
Breger M., 1975, Monthly Notes of the Astronomical Society of South Africa, 34, 76
Breger M., 1990, Delta Scuti Star Newsletter, 2, 13
Breger M., 2000a, Baltic Astronomy, 9, 149
Breger M., 2000b, in Breger M., Montgomery M., eds, Astronomical Society of the Pacific Conference Series Vol. 210, Delta Scuti and Related Stars. p. 3
Breger M., et al., 1993, A&A, 271, 482
Breger M., Pamyatnykh A., Pikall H., Garrido R., 1998, arXiv preprint astro-ph/9811338
Breger M., et al., 1999, Astronomy and Astrophysics, 349, 225
Breger M., et al., 2011, Monthly Notices of the Royal Astronomical Society, 414, 1721
Butters O. W., et al., 2010, A&A, 520, L10
Castelli F., 2003, in Symposium-International Astronomical Union. pp 47–48
Claret A., Hauschildt P., 2003, Astronomy & Astrophysics, 412, 241
Cox A. N., 2000, Allen's astrophysical quantities. Springer
Dupret M.-A., De Ridder J., De Cat P., Aerts C., Scuflaire R., Noels A., Thoul A., 2003, Astronomy & astrophysics, 398, 677
Fernley J., Jameson R., Sherrington M., 1984, Monthly Notices of the Royal Astronomical Society, 208, 853
Fitch W. S., 1981, ApJ, 249, 218
Gaia Collaboration et al., 2016, A&A, 595, A1
Gaia Collaboration et al., 2018, A&A, 616, A1
Ganesh S., Baliyan K., Chandra S., Joshi U., Kalyaan A., Mathur S., 2013, in Astronomical Society of India Conference Series.
Garrido R., 2000a, in The Third MONS Workshop: Science Preparation and Target Selection. p. 103
Garrido R., 2000b, in Breger M., Montgomery M., eds, Astronomical Society of the Pacific Conference Series Vol. 210, Delta Scuti and Related Stars. p. 67 (`arXiv:astro-ph/0001064`)
Garrido R., Garcia-Lobo E., Rodriguez E., 1990, Astronomy and Astrophysics, 234, 262

Gazeas K., Niarchos P., Boutsia K., 2004, Communications in Asteroseismology, 144, 26
Handler G., 2008, Communications in Asteroseismology, 157, 106
Handler G., et al., 2006, MNRAS
Hartman J., 2012, Astrophysics Source Code Library
Heynderickx D., 1994, Astronomy and Astrophysics, 283, 835
Jenkins J. M., et al., 2016, in Software and Cyberinfrastructure for Astronomy IV. p. 99133E
Joshi S., Joshi Y. C., 2015, Journal of Astrophysics and Astronomy, 36, 33
Joshi S., et al., 2012, MNRAS, 424, 2002
Joshi S., et al., 2016, A&A, 590, A116
Joshi S., Semenko E., Moiseeva A., Sharma K., Joshi Y. C., Sachkov M., Singh H. P., Yerra B. K., 2017, MNRAS, 467, 633
Kurtz D. W., Saio H., Takata M., Shibahashi H., Murphy S. J., Sekii T., 2014, Monthly Notices of the Royal Astronomical Society, 444, 102
Kurtz D. W., Shibahashi H., Murphy S. J., Bedding T. R., Bowman D. M., 2015, Monthly Notices of the Royal Astronomical Society, 450, 3015
Kurucz R., 1993, ATLAS9 Stellar Atmosphere Programs and 2 km/s grid. Kurucz CD-ROM No. 13. Cambridge, 13
Langford W. R., 1976, PhD thesis, Brigham Young Univ., Provo, UT.
Lenz P., Breger M., 2004, in Zverko J., Ziznovsky J., Adelman S. J., Weiss W. W., eds, IAU Symposium Vol. 224, The A-Star Puzzle. pp 786–790, doi:10.1017/S1743921305009750
Li L.-J., Qian S.-B., 2013, PASJ, 65, 116
Luri X., et al., 2018, A&A, 616, A9
Moffett T. J., Barnes III T. G., Fekel Jr F. C., Jefferys W. H., Achtermann J. M., 1988, The Astronomical Journal, 95, 1534
Pamyatnykh A. A., 1999, Acta Astron., 49, 119
Paparó M., Szeidl B., Mahdy H. A., 1988, Astrophysics and space science, 149, 73
Paxton B., Bildsten L., Dotter A., Herwig F., Lesaffre P., Timmes F., 2011, ApJS, 192, 3
Paxton B., et al., 2013, ApJS, 208, 4
Paxton B., et al., 2015, ApJS, 220, 15
Paxton B., et al., 2018, ApJS, 234, 34
Paxton B., et al., 2019, ApJS, 243, 10
Pollacco D. L., et al., 2006, PASP, 118, 1407
Ricker G., Winn J., Vanderspek R., 2015, Inst. Systems, 1, 014003
Rogers F. J., Iglesias C. A., 1996, in American Astronomical Society Meeting Abstracts #188. p. 915
Soliman M., Hamdy M., Szeidl B., Szabados L., 1986, Commmunications of the Konkoly Observatory Hungary, 88, 39
Stellingwerf R. F., 1979, ApJ, 227, 935
Strassmeier K. G., Boyd L. J., Epand D. H., Granzer T., 1997, PASP, 109, 697
Suárez J., Garrido R., Goupil M., 2006, Astronomy & Astrophysics, 447, 649
Suárez J., Hernández A. G., Moya A., Rodrigo C., Solano E., Garrido R., Rodón J., 2014, Astronomy & Astrophysics, 563, A7
Torres G., 2010, AJ, 140, 1158
Uytterhoeven K., et al., 2011, Astronomy & Astrophysics, 534, A125
Van Genderen A., 1967, Bulletin of the Astronomical Institutes of the Netherlands, 19, 74
Watson R., 1988, Astrophysics and Space Science, 140, 255
Zechmeister M., Kürster M., 2009, A&A, 496, 577

This paper has been typeset from a TEX/LATEX file prepared by the author.